International Journal of Medical Microbiology 309 (2019) 351–358

Contents lists available at ScienceDirect

International Journal of Medical Microbiology

journal homepage: www.elsevier.com/locate/ijmm

Structural diversity of coiled coils in protein fibers of the bacterial cell envelope

Birte Hernandez Alvarez*, Jens Bassler, Andrei N. Lupas*

Department of Protein Evolution, Max Planck Institute for Developmental Biology, Max-Planck-Ring 5, 72076, Tübingen, Germany

ARTICLE INFO

Keywords:
Coiled coil
Polar core
β-layer
Trimeric autotransporter adhesin

ABSTRACT

The cell envelope of bacteria shows great diversity in architecture and composition, to a large extent due to its proteome. Proteins localized to the cell envelope, whether integrally embedded in the membrane, membrane-anchored, or peripherally associated as part of a macromolecular complex, often form elongated fibers, in which coiled coils represent a prominent structural element. These coiled-coil segments show a surprising degree of structural variability, despite being shaped by a small number of simple biophysical rules, foremost being their geometry of interaction referred to as 'knobs-into-holes'. Here we will review this diversity, particularly as it has emerged over the last decade.

1. Introduction

Cell envelopes are highly complex structures that protect cells from the environment, impart stability, facilitate compartmentalization and provide matrices for biological processes. Many of the proteins localized at the bacterial cell envelope form elongated fibers, either arrayed along the membrane, or protruding from the cell surface. Such protein fibers constitute a functionally and structurally heterogeneous group of proteins, which may provide elasticity and stability to the cell, project functional domains across large distances, or mediate processes like biofilm formation, the exchange of solutes with the environment, and host colonialization.

Depending on whether their preponderant secondary structure is α-helix or β-sheet, the domains forming these proteins can be categorized as α-fibrous or β-fibrous, a general rule of thumb being that monomeric proteins are formed of β-fibrous domains, whereas oligomeric ones may be α-fibrous, β-fibrous, or a combination thereof. In addition, collagen-like domains formed by polyglycine type II helices have been detected in increasing numbers in trimeric surface proteins (Lukomski et al., 2017; Yu et al., 2014), where they appear to be flanked mainly by α-fibrous domains (see for example Squeglia et al., 2014). β-Fibrous structural motifs include a wide range of forms: continuous spirals of right-handed or left-handed β-helices (Kajava et al., 2006), but also chains of discrete domains, primarily with an immunoglobulin-like fold (Bodelon et al., 2013). In contrast, there is essentially only one α-fibrous motif found in non-membrane embedded domains of bacterial cell envelope proteins, the coiled coil.

Indeed, the coiled coil was first proposed on the basis of X-ray diffraction spectra of protein fibers, albeit of animal origin (Astbury, 1938). These data independently led Francis Crick and Linus Pauling to describe bundles of α-helices winding around each other as the main structural element of these proteins (Crick, 1952; Pauling and Corey, 1953). Particularly the detailed parametric model of Crick (Crick, 1953a), derived from a specific representation of side-chain packing interactions (Crick, 1953b), became established as the canonical account of the coiled coil. This model was based on the realization that α-helices interacting at an angle of about 20° would be able to interlock their side-chains regularly in a geometric pattern repeating every seven residues (or two turns of the helix). Francis Crick described this interlocking of residues as ‘knobs’ into ‘holes’ and proposed that the energy needed to distort the α-helices, such that the crossing angle could be maintained over large distances, resulted from the hydrophobic effect, deducing that coiled coils would show a sequence periodicity of seven residues (the heptad repeat), with hydrophobic residues in the first and fourth position forming the knobs-into-holes interactions. Although it took more than a quarter-century, this model was fully confirmed by experimental data and coiled coils became synonymous with simple, very regular structures mediating oligomerization and mechanical stability (Lupas and Gruber, 2005; Squire and Parry, 2017). More recently, particularly over the last decade, it has become apparent, however, that coiled coils are functionally much more versatile (Hartmann, 2017; Lupas et al., 2017) and that this versatility is underpinned by a surprising range of structural variants. While fully compatible with Crick's model, these variants highlight the possibilities inherent in a seemingly

* Corresponding authors at: Department of Protein Evolution, Max Planck Institute for Developmental Biology, Max-Planck-Ring 5, D-72076, Tübingen, Germany.
E-mail addresses: birte.hernandez@tuebingen.mpg.de (B. Hernandez Alvarez), andrei.lupas@tuebingen.mpg.de (A.N. Lupas).

https://doi.org/10.1016/j.ijmm.2019.05.011
Received 23 January 2019; Received in revised form 14 April 2019; Accepted 31 May 2019

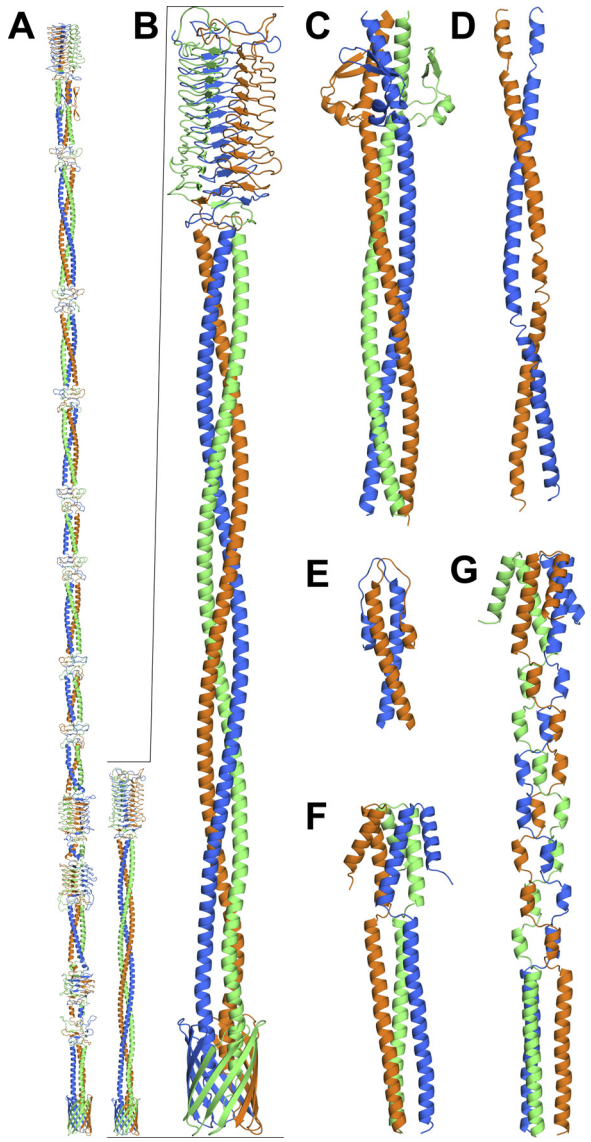

Fig. 1. Structural diversity of coiled-coil fibers. (A) Structural models of the complex TAA SadA from Salmonella Typhimurium (left) (Hartmann et al., 2012) and prototypic TAA *Yersinia enterocolitica* YadA (right) (Koretke et al., 2006). **(B)** Enlarged view of the YadA model. **(C)** Crystal structure of the head domain and the N-terminal stalk region of the TAA NadA3 from *Neisseria meningitidis* (PDB: 6EUN). **(D)** Crystal structure of the BC1 fragment of M protein from *Streptococcus pyogenes* (PDB: 2XNX). **(E)** Crystal structure of the N-terminal domain of *Bacillus subtilis* DivIVA (PDB: 2WUJ). **(F, G)** Model structures of the soluble fragments of mempromCC homologs from *Caulobacter crescentus* NA1000 (YP_002517927) and *Caulobacter* sp. JGI 0001013-D04 (WP_018113394) (Adlakha et al., 2019). All proteins are homo-oligomers with their single chains colored in different levels of gray.

rigid set of rules. Structural studies of protein fibers of the bacterial cell envelope were instrumental in revealing this versatility and, in this review, we provide an overview of these proteins with a focus on the structural diversity of their coiled-coil domains.

2. Diversity of coiled-coil fibers in domain architecture and function

Coiled-coil fibers of the bacterial cell envelope form a heterogeneous group of proteins belonging to different protein families, among them the most prominent family of trimeric autotransporter adhesins (TAAs) that has been studied intensively within the last decade (Lyskowski et al., 2011). Other families comprising coiled-coil proteins at the cell envelope include homologs of M protein, the major virulence determinant of *Streptococcus pyogenes* (Fig. 1) (Ghosh, 2018; Kelemen, 2017), intermediate Filament (IF)-like proteins (Kelemen, 2017), homologs of the cell division protein DivIVA from Gram-positive bacteria (Oliva et al., 2010), and prokaryotic members of the most recently discovered mempromCC family (*membrane-bound proteins from prokaryotes and mitochondria containing coiled coils)* (Adlakha et al., 2019).

TAAs constitute the largest of these families. Mainly present in proteobacteria, this family includes many pathogenicity and virulence factors, such as YadA from *Yersinia enterocolitica*, BadA from *Bartonella henselae* and XadA from the plant pathogen *Xanthomonas campestris* (Linke et al., 2006). TAAs are homotrimers that consist of an N-terminal passenger domain and an evolutionarily conserved C-terminal translocator domain, which defines the family. The translocator domain assembles into a twelve-stranded β-barrel, which, spanning the outer membrane, anchors the protein. The extracellular passenger domain occludes the pore of the barrel. It is rich in coiled-coil structure and highly variable in length and subdomain composition. Analyzing the chain length, we find the vast majority of TAAs to comprise between 300 and 2000 residues, with the shortest known TAA, BN80_143 identified from the *Yersinia* phage phiR1 RT comprising 122 residues, and the longest, B11Cv2_001710 from *Bartonella* sp. *1-1c* consisting of 7883 residues (Bassler et al., 2015). Representing rather small fibers, YadA from *Y.enterocolitica* (Hoiczyk et al., 2000; Koretke et al., 2006) and NadA5 from *Neisseria meningitidis* (Malito et al., 2014), comprise 422 and 325 residues and reach lengths of 33 nm and 27 nm, respectively. Exemplary for prototypic TAAs, YadA forms lollipop-like structures on the cell surface (Hoiczyk et al., 2000) and follows a simple head-stalk-anchor architecture with an N-terminal globular head domain projected by an elongated coiled-coil stalk that proceeds at the C-terminus in the membrane anchor (Fig. 1A, B). Compared to such rather simply structured adhesins, many family members of the TAA family constitute complex fibers showing a high degree of modularity. Applying a “Divide-and-conquer” approach, we solved the crystal structures of multiple segments of the complex adhesin SadA from Salmonella Typhimurium (*Salmonella enterica ssp. enterica serovar Typhimurium*), based on which we reconstructed structural models of the whole fiber of SadA as well as its orthologs UpaG and EhaG from uropathogenic and enteropathogenic *Escherichia coli* strains (Fig. 1A) (Hartmann et al., 2012). In general, the size of coiled-coil segments in TAAs varies from a single 7-residue repeat, seen in the *Haemophilus influenzae* adhesin Hia (see PDB: 1S7M, 107-VGDLRG-112) (Yeo et al., 2004), up to more than a thousand residues in the hemagglutinin-like outer membrane protein of *Burkholderia* sp. 383 (YP_371201). The rigidity and elongated shape of the coiled-coil segments contribute significantly to the length and stiffness of TAA fibers. In YadA, the stalk domain accounts with 136 residues for roughly a third of the length of the passenger domain; whereas in the folded trimer, it takes more than three quarter of the exposed protein length (Hoiczyk et al., 2000). The passenger domains are highly adhesive and mediate attachment to other bacteria, promoting biofilm formation and microcolonialization, but also to abiotic surfaces, including plastics and glass (Ishikawa et al., 2012; Lazar Adler et al., 2013; Raghunathan et al., 2011; Ruiz-Ranwez et al., 2013). As essential virulence factors during early steps of infection and host colonialization, TAAs of many pathogens target extracellular matrix molecules, like collagen, fibronectin and vitronectin as well as receptors, such as CEACAM1 and TNFR1 (Conners et al., 2008; Hill et al., 2015; Leduc et al., 2009; Leo et al., 2008; Mil-Homens et al., 2017; Singh et al., 2014). TAAs induce inflammatory processes and apoptosis (Wang et al., 2016), but also evade host defense by mediating serum resistance through inhibition of complement attack and phagocytosis (Leduc et al., 2009; Singh et al., 2014; Sjolinder et al., 2008).

As the major surface antigen of the Gram-positive bacterial pathogen *S. pyogenes*, the M protein constitutes with more than 200

serotypes another intensively studied coiled-coil surface fiber. Mature M proteins comprise about 320–440 residues and appear as a dense coat of protruding fibrillary structures, about 50 nm in length, on the cell surface (Phillips et al., 1981; Smeesters et al., 2010). They form a continuous dimeric parallel coiled coil that is covalently linked to the peptidoglycan layer via its C-terminus (Fig. 1D). The rod of mature M protein is divided in four repeat domains (A, B, C, and D), which differ in size and sequence. The N-terminal 40-50 residues constitute a hypervariable region that is followed by the less variable A and B repeats and, finally at the C-terminus, by the highly conserved C and D repeat domains. Based on their sequence variability, different M protein serotypes bind different host molecules, including fibrinogen, plasminogen, complement factors and immunoglobulins, confer fibrinolysis and resistance against phagocytosis or show proinflammatoric properties (Ghosh, 2018).

Intermediate filament (IF)-like proteins constitute a group of coiled-coil fibers that share the domain architecture of eukaryotic IFs, but are more variable in sequence and function. They comprise a central elongated coiled-coil domain, which is composed of three conserved coiled-coil motifs and flanked by two small globular domains. Similar to their eukaryotic counterparts, bacterial IF-like proteins at the cell envelope form filamentous networks that mechanically stabilize the cells, supporting cell shape, growth and division (Kelemen, 2017). Crescentin, the most intensively studied IF-like protein from Gram-positive bacteria, is essential for curvature formation in *Caulobacter crescentus* and forms filamentous structures at the inner membrane curvature of crescent-shaped cells (Briegel et al., 2006). Binding of a stretch of positively charged residues at the N-terminus of crescentin to the membrane is assumed to generate a mechanic force affecting the rate of peptidoglycan synthesis and regulating cell shape (Cabeen et al., 2009). The tripartite domain architecture of crescentin resembles that of eukaryotic IFs. Its elongated α-helical rod forms a parallel dimeric coiled coil and plays a key role in filament assembly. With a length of 365 residues, the rod constitutes the major part of the protein having a total length of 440 residues (Cabeen et al., 2009).

Scy and FilP represent two other IF-like fibers from the Actinobacterium *Streptomyces coelicolor*. In contrast to other IF-like proteins, both proteins comprise a central rod that is built from only two coiled-coil motifs connecting two rather small globular domains (Walshaw et al., 2010). Scy and FilP homologs localize to the membranes at polar growth zones in *Streptomycetales* and *Actinomycetales*, where they constitute scaffolds for multiprotein assemblies during polar cell wall biogenesis (Fuchino et al., 2013; Holmes et al., 2013).

DivIVA is one of the proteins that associate with Scy and FilP to trigger polar cell growth in *Streptomyces* species (Holmes et al., 2013). Widely spread in Gram-positive bacteria, DivIVA homologs lack any globular domain and form parallel dimeric coiled coils built from two α-helical domains connected by a variable linker (Fig. 1E). From structural studies of *Bacillus subtilis* DivIVA, the dimers are suggested to assemble into filamentous structures by oligomerization of their C-terminal coiled-coil segments (Oliva et al., 2010). DivIVA homologs regulate cell shape and, similar to Scy and FilP, they specifically localize to sites of cell wall synthesis, including tips and branching sites of hyphae in *Actinobacteria* as well as cell poles and division septa in non-filamentous bacteria (Kelemen, 2017).

Prokaryotic members of the mempromCC family represent another group of proteins that are widespread in proteobacteria and form thin elongated structures of variable length at the cytoplasmic membrane (Fig. 1F, G). They follow a tripartite domain architecture comprising a conserved helical head domain that is projected by a C-terminally membrane-anchored coiled-coil stalk (Adlakha et al., 2019). The coiled coils of mempromCC homologs are highly diverse in sequence and variable in length, ranging from about 60–120 residues. In contrast to their human and yeast homologs functioning as assembly factors and/or scaffolds for multiprotein complexes in the inner mitochondrial membrane (Paupe et al., 2015; Tomar et al., 2016), bacterial mempromCC homologs are functionally uncharacterized so far.

The wide spectrum of biological functions of coiled-coil fibers at the bacterial cell envelope as well as their variability in domain composition and architecture - briefly described here - is to a large extent based on the structural properties and peculiarities of their coiled-coil segments, which will be reviewed in the following.

3. Structural diversity of coiled coils in bacterial cell surface fibers

3.1. Polar cores

In canonical coiled coils, the amino acid sequence of the constituent helices shows a periodicity of hydrophobic and hydrophilic residues, which repeats every 7 residues (the heptad repeat). If the seven positions of this repeat are labeled *a–g*, positions *a* and *d* are usually occupied by hydrophobic residues, which point their sidechains towards the central axis of the coiled coil, forming the core of the bundle. Many bacterial surface fibers depart from this rule in order to systematically project hydrophilic residues into the core, often as part of conserved polar sequence motifs (Bassler et al., 2015).

Especially in stalks of TAAs, we frequently find fragments in which canonical heptad repeats are interspersed with segments predicted to be unstructured (Hartmann et al., 2009). In these regions, the heptad repeat pattern of the flanking coiled is continued, but the core positions *a* and *d* are occupied by an unusual high percentage of polar or charged residues. Coiled coils, in general, contain polar residues in about a quarter of their core positions with the highest incidence in dimeric coiled coils, where core residues are comparatively more solvent exposed (Akey et al., 2001). Studies with the dimerization domain of the yeast transcription factor GCN4 showed polar core residues to decrease coiled-coil stability, but also to impart specificity (Knappenberger et al., 2002). In TAAs, the number of consecutive repeats containing polar core residues is highly variable, ranging from single repeats, as they are present in SadA, up to 37 repeats found in a hypothetical TAA from *Brucella microti* (WP_015799745). About 50% of heptad repeats from TAAs contain a residue with charged or polar sidechains in position *d*, such as N, T, Q, D and H, preceded by a hydrophobic residue in position *a*. So called N@*d* layers, with asparagine occupying position *d*, are most frequently found within heptads of the sequence [I/V]xxNTxx, with a hydrophobic residue in the preceding position *a* and followed by T in over a half of the cases. We further identified repeats, like LxxTNxx, in which positions of N and T are reversed or, more rarely, both core positions are occupied by hydrophilic residues, such as in NxxQDxx, SxxNTxx, QxxHxxx, and QxxDxxx (Hartmann et al., 2009).

In a structural and biophysical study, we comprehensively characterized N@*d* motifs from the complex *S. typhimurium LT2* adhesin SadA containing six coiled-coil fragments with consecutively arranged IxxNTxx repeats (Fig. 2A) (Hartmann et al., 2009). In the crystal structure of one of these SadA stalk fragments, comprising residues 479–519, the sidechains of the asparagines in *d* point inwards forming the core of the coiled coil and, together with the succeeding threonines, they build an elaborate network of specific interactions coordinating chloride ions and nitrate in the center. Equally, bound anions were identified in N@*d* layers of structurally characterized stalk segments from *N. meningitidis* NadA (Malito et al., 2014), *Acinetobacter* sp. *Tol 5* AtaA (Koiwai et al., 2016), *Moraxella catarrhalis* UspA1 (Conners et al., 2008) and *E. coli* EibD (Leo et al., 2011). Furthermore, ion-coordinating arrangements, other than N@*d* layers, are found in the center of the EibD and UspA1 stalks. The stalk of UspA1 contains three histidines (H573, H584 and H629) in core position *d* with two of them coordinating phosphate ions in the crystal structure (Fig. 2B) (Conners et al., 2008). In EibD, a chloride ion is coordinated by a threonine (T382) in position *a*, and a water molecule is bound by a histidine (H421) in position *d* (Fig. 2C) (Leo et al., 2011). At lower pH values, protonation of the histidines in repeat position *d* clearly impaired the stability of the coiled coil in this region (Conners et al., 2008).

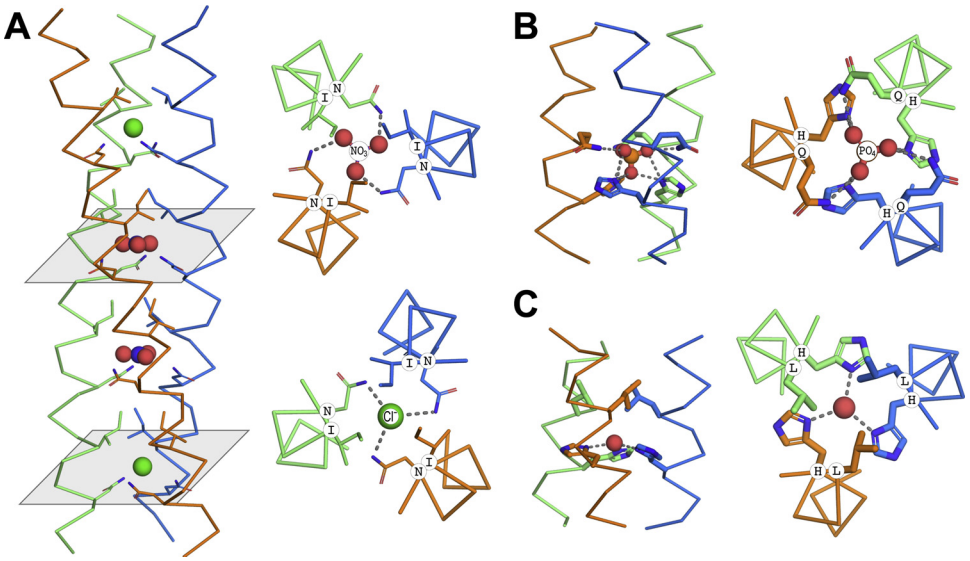

Fig. 2. Polar core motifs coordinating ions in coiled coils. (A) Side and top view of four consecutive IxxNTxx motifs from a coiled-coil stalk segment of Salonella Typhimurium SadA with the asparagines in position *d* (N@*d* layers) sequestering chloride and nitrate ions in the core (PDB: 2WPQ). **(B)** A QxxHxxx motif coordinating phosphate in the coiled-coil stalk of *Moraxella catarrhalis* UspA1 (PDB: 2QIH). **(C)** A histidine residue in position *d* of the coiled-coil stalk of EibD from *Escherichia coli* coordinating a water molecule in the center (PDB: 2XQH). In all panels, monomers are shown in different levels of gray. Core residues and coordinated ions are labeled in top view.

Similarly, we found the insertion of N@*d* layers in the trimeric leucine zipper variant GCN4-pII to progressively destabilize coiled-coil structure (Hartmann et al., 2009). In this context, N@*d* layers were also found to orient themselves specifically into the core and to fold at high local concentration. Based on these observations, we suggest that polar core residues in the coiled-coil stalks of TAAs constitute a destabilizing element, necessary to keep the single chains of the passenger domain in an unfolded state in the periplasm before and during export to the cell surface. Once, located outside the cell, the single chains align and fold specifically, presumably triggered by the folding of adjacent domains.

The functionality of the *S. pyogenes* M protein is also regulated by the stability of its dimeric coiled coil. Especially, the segment involved in fibrinogen binding, which encompasses the region of the B repeats, is surprisingly unstable under physiological conditions. It exist in four different states: an unfolded disordered state, a folded monomer and two dimeric coiled-coil states, the latter characterized by two alternate registers with different affinities for fibrinogen (McNamara et al., 2008; Stewart et al., 2016). This instability is based on irregularities in coiled-coil structure, including residue insertions or deletions in the heptad pattern, polar core residues, and so called Ala staggers that, consisting of alanine residues in successive core positions, locally change the coiled-coil radius. Some of these destabilizing elements are evolutionarily conserved and, as shown by mutational analysis, essential for the molecular dynamic of M protein, which in turn is a prerequisite for the interaction with human fibrinogen. It is assumed that a dynamic conformation of the coiled coil of M protein binds to fibrinogen, and finally upon binding, collapses into a second alternate, more stable register (Stewart et al., 2016).

3.2. Non-canonical periodicities

The 7-residue repeats of canonical coiled coils are arranged over two α-helical turns to yield a periodicity of 3.5 residues per turn (Fig. 3A). Like in many other natural proteins, the coiled coils of bacterial surface fibers frequently deviate from this standard model of periodicity, bringing about variations in the geometry of core packing and the handedness of the supercoil. These differences arise from insertions of residues into the heptad repeats. Additional single residues, so called skips, are accommodated either locally as kinks, constituting short π-helical segments, or delocalized over several repeats (Lupas and Gruber, 2005). Insertions of three and four residues, named stammers and stutters, respectively, are rather well tolerated within coiled-coil structure, as in either case the number of inserted residues corresponds to approximately one helical turn in a canonical coiled coil (Brown et al., 1996).

While the majority of coiled coils in TAAs constitute trimeric left-handed bundles based on a heptad repeat pattern, some TAAs also comprise stalk segments that are rather straight or even right-handed. Such segments contain single or repetitively arranged hendecads or pentadecads, constituting repeats of eleven and fifteen residues, respectively. Hendecads arise upon insertion of four residues in a heptad (7 + 4) and, accommodated over three helical turns, they unwind the bundle locally. With a periodicity of 3.67 (11/3), hendecad-based coiled coils adopt an undistorted to slightly right-handed conformation. In comparison, pentadecads contain two stutters per repeat (7 + 4 + 4 = 15) and are accommodated over four helical turns in a right-handed coiled coil with a periodicity of 3.75 (15/4).

Single hendecads embedded in heptad repeats are found for instance in the stalks of *N. meningitidis* NadA3 and *M.catarrhalis* UspA1, where they cause local unwinding of the coiled coil (Conners et al., 2008; Liguori et al., 2018). The N-terminal half of the stalk of the immunoglobulin binding TAA EibD from *E. coli* constitutes a slightly right-handed coiled-coil segment built from three consecutive hendecads (Fig. 3B) (Leo et al., 2011). The YadA stalk represents a vivid example of a pronounced right-handed coiled coil that, in dependence of the serotype, is composed of seven or nine pentadecads (Fig. 3C) (Hoiczyk et al., 2000; Koretke et al., 2006). As the pore of the membrane-anchored β-barrel in TAAs is invariably occluded by a canonical coiled coil, right-handed stalks switch their handedness to left-handed before entering the membrane. Solving the crystal structure of the corresponding YadA stalk fragment, we could show that this transition is facilitated through local unwinding by another unusual 19-residue repeat, connecting the last pentadecad with four canonical heptads (Fig. 3D) (Alvarez et al., 2010).

As identified from electron micrographs, a single hendecad in the stalk of Usp1 colocalizes with a bending site of the fiber (Conners et al., 2008). Interestingly, this region overlaps in the crystal structure with a large cavity in the surface of the stalk. Similar cavities have also been identified at potential bending sites in the stalks of YadA and EibD (Leo et al., 2011), which suggests a role in bending of stalk domains, a phenomenon that has been observed for many TAA fibers in different experimental approaches and is assumed to be important for function.

Right-handed coiled coils of TAAs, such as the mentioned YadA and EibD proteins, frequently contain single or multiple conserved YxD motifs in their sequence, with usually threonine in position x. Within this motif, the side-chains of the tyrosine and the aspartate form an extended network of inter-chain and intra-chain interactions, determining the oligomerization state and imparting stability (Alvarez

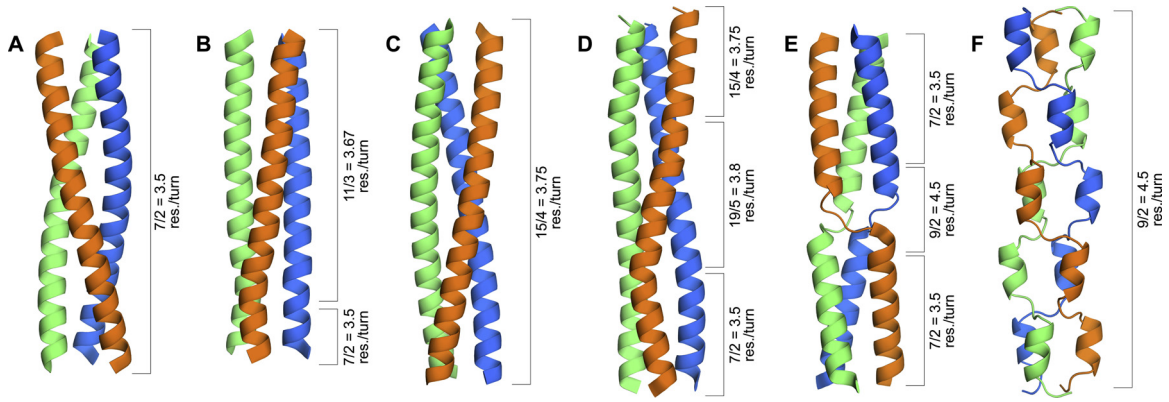

Fig. 3. Coiled-coil periodicities in TAAs. (A) A canonical left-handed coiled-coil segment from the stalk of Salmonella Typhimurium SadA (PDB: 2WPQ) accommodating seven residues over two helical turns (7/2). **(B)** Fragment of the EibD stalk domain showing a transition from slightly right-handed hendecads (11/3) to left-handed heptads (7/2) (PDB: 2XQH). **(C)** A coiled-coil segment of strongly right-handed pentadecad (15/4) periodicity in the modelled structure of YadA (Koretke et al., 2006). **(D)** Transition from right-handed to left-handed supercoiling mediated by a 19/5 segment in YadA (PDB: 3LT7). **(E)** Fragment of the coiled-coil stalk domain of OMP100 from *Actinobacillus actinomycetemcomitans* containing a single β-layer built from a nonad (3 + 3+3) (PDB: 5APP). **(F)** Stalk-neck region of the mempromCC homolog from *Caulobacter* sp. JGI 0001013-D04 (WP_018113394) comprising consecutive nonads that form repetitive β-layers, which alternate with α-helical structure (Adlakha et al., 2019).

et al., 2010). In most YxD motifs, the central x-residue occupies position *l* of the pentadecad (*a-b-c-d-e-f-g-h-i-j-k-l-m-n-o*). EibD contains a rare version of YxD with the x occupying position *a* (Leo et al., 2011; Szczesny and Lupas, 2008). YxD motifs are specific for right-handed coiled coils and constitute the equivalent of the RxD motif, which forms comparably stabilizing interaction networks in left-handed coiled coils (Kammerer et al., 2005).

Non-canonical periodicities are not restricted to TAAs, they are also found in bacterial IF-like fibers. The helical rod of structurally uncharacterized Crescentin shows a canonical heptad repeat pattern that is disrupted by a single stutter (hendecad) at the C-terminal end. A mutant lacking this stutter is largely affected in filament formation and, upon expression in *C. crescentus*, diffusely delocalizes throughout the cytoplasm and interferes with cell curvature formation (Cabeen et al., 2011). Similarly, deletion of a stutter in the same region of eukaryotic vimentin affected filament formation, but not dimerization of the coiled coil (Herrmann et al., 1999).

The structurally very similar rods of IF-like proteins FilP and Scy are composed of two distinct coiled-coil sub-domains of different periodicities. The shorter N-terminal sub-domain is built from canonical heptad repeats; whereas the longer C-terminal coiled coil comprises of unusual 51-residue repeats (penindaenads) built from single heptads succeeded by four hendecads (7-11-11-11-11) (Walshaw et al., 2010). Based on biochemical data, FilP and Scy are likely to form straight dimeric coiled coils, capable to assemble in higher order filamentous structures. The spatial arrangement and orientation of single filaments within these assemblies is speculation so far, as there is no structural data available for both, the proteins as well as the filamentous arrays formed by both proteins and mutants thereof (Kelemen, 2017).

In prokaryotic homologs of the mempromCC family, the coiled coils forming the stalk are highly diverse in periodicity, even between closely related species. They are predominantly built from canonical heptads and hendecads, but occasionally contain pentadecads and repeats of odd length, some of which even break coiled-coil structure and form β-layers, a structural element in coiled coils described below.

3.3. β-layers

Performing sequence analysis of coiled-coil segments, we occasionally identified extreme departure from canonical heptad periodicity. For instance in some TAA stalks, we observed repeats of unusual length embedded within canonical heptads, namely hexads and nonads comprising of six and nine residues, respectively (Hartmann et al., 2016). These repeats can be considered as two (3 + 3 = 6) and three (3 + 3+3 = 9) consecutive stammers, which are rather rarely found in coiled coils compared to the more frequently occurring stutters. A single stammer (7 + 3 = 10) introduced in a canonical coiled coil locally overwinds the bundle, leading to a periodicity of 3.33 (10/3) and, in some cases, to the formation of short 3_{10}-helical segments (Brown et al., 1996; Hartmann et al., 2009). We structurally characterized a stalk segment of the TAA OMP100 *from Actinobacillus actinomycetemcomitans*, comprising a nonad flanked by canonical heptads, and found that these types of insertions break coiled-coil structure (Fig. 3E). The strain that is put on the single helices at the site of insertion causes their breakage and leads to the formation of a β-layer, a triangular supersecondary structural element arranged perpendicular to coiled-coil axis (Hartmann et al., 2016). β-Layers comprise three short β-strands, each built from three residues of each chain of the trimer, that finally switch back to α-helical structure with the monomers shifted 120° around coiled-coils axis counterclockwise (ccw) as seen from the N-terminus. β-Layers are stabilized by specific backbone interactions: the first formed between the central β-layer residues across the trimer, and the second built across the chains between the residue in the preceding position *c* and the successive residue in position *e* of the neighboring chain. Analyzing hexad and nonad insertions in the background of the trimeric leucine zipper variant GCN4-pII, we found β-layers to invariably arise in repeat position *d* and showed that conversion of hexads and nonads into canonical heptads restores a continuous coiled coil. β-Layers occur as single elements or repetitively arranged, forming α/β coiled coils, a type of protein fiber with alternating α/β structure (Figs. 3F and 4).

The identification of β-layers from sequence is difficult, as they are built from irregular repeats, which usually evade recognition by prediction tools. For that reason, we manually performed sequence searches to identify β-layers using conserved β-layer sequence motifs as search templates. The majority of β-layers has been identified so far in TAAs and members of the mempromCC family; where they are found either flanked by coiled-coil segments or located at their ends, serving as connectors for adjacent domains (Fig. 4) (Adlakha et al., 2019; Hartmann et al., 2012, 2016).

Although, there is no functional information for β-layers so far, their structural importance is fairly clear. Embedded within a coiled coil, β-layers increase its resilience to harsh conditions by tightly interweaving its monomers and preventing dissociation and aggregation. Furthermore as universal domain adaptors, they likewise contribute to fiber complexity and probably provide a certain degree of flexibility to

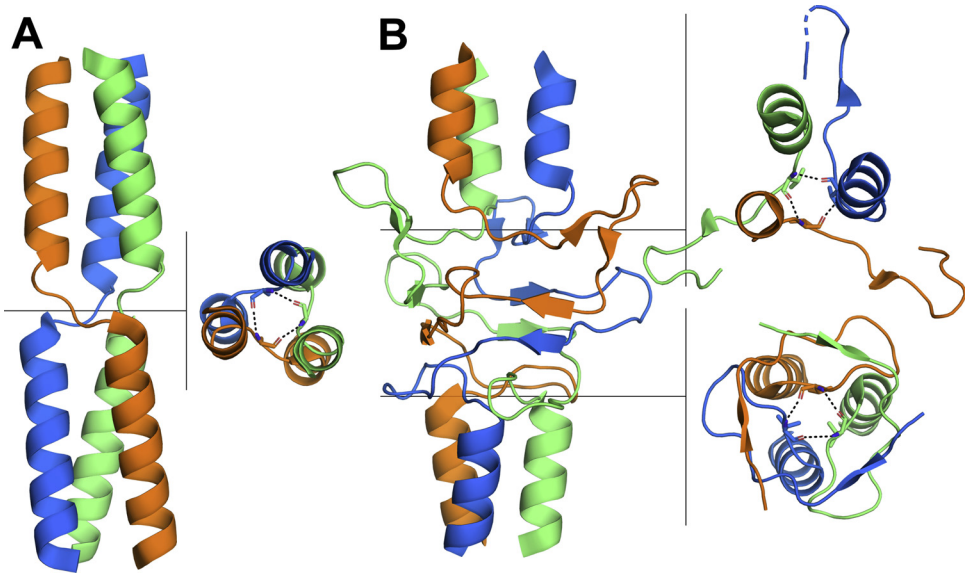

Fig. 4. β-layers as connectors of α-helical and β-stranded secondary structure. (A) Side and top view of a single β-layer resulting from a nonad embedded in the coiled-coil stalk of *Actinobacillus actinomycetemcomitans* OMP100 (PDB: 5APP). **(B)** A DALL domain of Salmonella Typhimurium SadA flanked by two β-layers (PDB: 2YO3). The N-terminal β-layer (upper right panel) facilitates the direct transition from the coiled coil into the first β-strand of the DALL domain. As part of the neck, the C-terminal β-layer (lower right panel) mediates the transition from the β-structured DALL domain into the succeeding coiled coil. In **(A)** and **(B)**, top views show the backbone hydrogen bonds that are formed between the central β-layer residues of the three monomers across the trimer.

adjacent domains (Adlakha et al., 2019).

3.4. Minidomain insertions

In complex TAAs, the coiled-coil stalk segments connect multiple globular domains, differing in size and architecture. As discussed previously (Bassler et al., 2015), some of these are comparably small in size and reminiscent of insertions rather than of domains, which makes a clear classification difficult in many cases. In the following, these types of insertions/domains are referred to as minidomains, a term already used before (Leo et al., 2011).

FGG domains representing such a type of insertion are found in coiled coils of TAAs. They comprise about 50–55 residues and most frequently contain a conserved LGG motif instead of the name-giving FGG motif. They comprise two β-hairpins flanked by short helical fragments, which, stabilized by a tight interaction network, fit the coiled-coil stalk like a collar (Fig. 5A). They seamlessly proceed in coiled-coil structure, moving the path of the single chains 120° ccw around coiled-coil axis, suggesting a stabilizing function.

The headCap constitutes a second type of peripheral hairpin insertion in a coiled coil that, as the name says, forms a cap-like structure on top of the subsequent head domain (Fig. 5B). It shows a α_1-β_1-β_2-α_2-β_3-β_4-β_5-β_6-α_3 topology comprising three β-hairpins that are held together by an α-helical core with the α_1 helix and the β_5-β_6 hairpin sharing homology to FGG minidomains (Koiwai et al., 2016). headCaps form an elaborate interchain interaction network and, like FGG minidomains, they translocate the chains of the monomers 120° ccw.

The saddle, which has only been identified in *E. coli* EibD so far, comprises 22 residues forming three short antiparallel β-sheets that are stabilized by an ion-coordinating interaction network at the exit and re-entry points of the stalk (Fig. 5C). The identification of this insertion was rather surprising, as there was no indication for this type of structure from sequence, which was predicted to form a continuous coiled coil. In the structure, the saddle connects the N-terminal right-

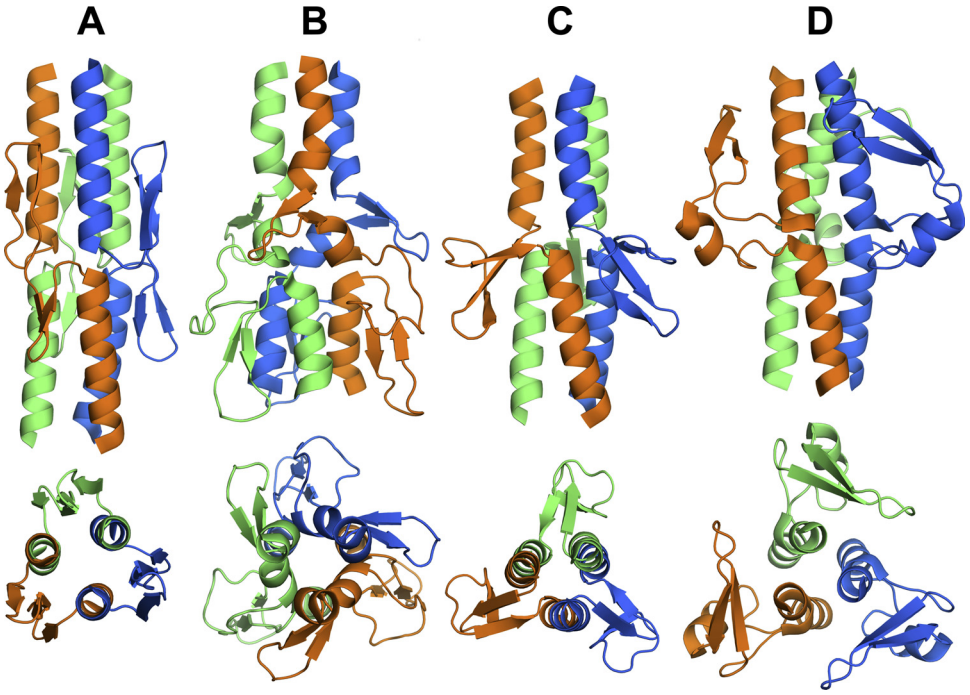

Fig. 5. Minidomain insertions in coiled coils of TAAs. Side and top views of minidomain insertions found in TAAs including **(A)** the FGG domain inserted in the coiled-coil stalk of SadA (PDB: 2YNY), **(B)** the headCap of *Acinetobacter* sp. *Tol 5* (PDB: 3WP8), **(C)** the saddle of EibD (PDB: 2XQH), and **(D)** the minidomain insertion in NadA3 from *Neisseria meningitidis* (PDB: 6EUN).

handed stalk segment with the C-terminal left-handed segment, thereby, similar to FGG and headCap, moving the path of the monomers 120° around coiled-coil axis. Thus, this minidomain represents an alternative way to the 19-residue fragment in the YadA stalk facilitating a switch in handedness in coiled coils (Leo et al., 2011; Alvarez et al., 2010).

Another vivid example for a minidomain is the head region of NadA3 from *N. meningitides*. Originally predicted to comprise an elongated coiled-coil stalk domain with an N-terminally embedded head domain, the crystal structure of NadA3 shows the N-terminus to equal an coiled coil disrupted by a minidomain-like insertion (Fig. 5D) (Liguori et al., 2018).

4. Conclusion

The structure of coiled coils is highly regular and rigid, which, at a first glance, seems to leave little space for variability. However, the work that has been done on the characterization of coiled coils until today has proved the opposite, showing that the functional diversity of coiled coils is to a large scale based on their structural versatility.

Coiled coil-containing protein fibers at the bacterial cell envelope contribute to stability, mediate adhesion and regulate cell shape and growth. Like other naturally occurring coiled coils, they frequently deviate from the canonical standard model and show peculiarities in sequence and structure. As reviewed here, they exploit various strategies to meet special functional requirements within the constraints of coiled-coil structure. Serving as connectors or projectors for other domains, they are usually less conserved in sequence, but comprise of a highly regular repeat pattern, which provides the required stability of coiled-coil structure. Contrarily, other coiled coils seem rather to walk on a tightrope between functionality and stability, such as TAA stalks, which tolerate long stretches of destabilizing polar core residues in their coiled coils to facilitate the export of long chains to the cell surface. Another vivid example is represented by the *S. pyogenes* M protein using local instability in coiled-coil structure as a requirement for ligand binding. Furthermore, coiled-coil domains of protein fibers utilize different types of insertions to increase stability and modularity of the fiber as well as to trigger filament formation.

Most fibrous proteins are not amenable to structure determination by conventional methods and remain uncharacterized to date. However, the rather few examples of coiled coils from protein fibers at the bacterial cell surface that have been structurally characterized so far, already give a foretaste of a remarkable diversity. Given the rapidly advancing development of new techniques, such as Cryo-Electron Microscopy, the structural characterization of many more protein fibers can be anticipated in near future and will most likely continue to expand the spectrum of their structural variability.

Declarations of interest

None.

Acknowledgements

We thank our collaborators within the SFB “The bacterial cell envelope: Structure, Function, and Infection Interface” for helpful discussion and support. We are especially grateful to Dirk Linke (University of Oslo), Ingo Autenrieth (Tübingen University), Volkhard Kempf (University Hospital Frankfurt), Adrian Goldman (University of Leeds) and Katsutoshi Hori (University of Nagoya) for the fruitful long-term collaboration on the TAA project. This work was supported by the German Research Foundation (SFB766 B04) and institutional funds of the Max Planck Society.

References

Adlakha, J., Karamichali, I., Sangwallek, J., Deiss, S., Bar, K., Coles, M., Hartmann, M.D., Lupas, A.N., Hernandez Alvarez, B., 2019. Characterization of MCU-Binding proteins MCUR1 and CCDC90B - representatives of a protein family conserved in prokaryotes and eukaryotic organelles. Structure 27, 464–475.

Akey, D.L., Malashkevich, V.N., Kim, P.S., 2001. Buried polar residues in coiled-coil interfaces. Biochemistry 40, 6352–6360.

Alvarez, B.H., Gruber, M., Ursinus, A., Dunin-Horkawicz, S., Lupas, A.N., Zeth, K., 2010. A transition from strong right-handed to canonical left-handed supercoiling in a conserved coiled-coil segment of trimeric autotransporter adhesins. J. Struct. Biol. 170, 236–245.

Astbury, W.T., 1938. The fourth Spiers memorial lecture. X-ray adventures among the proteins. Trans. Faraday Soc. 34, 378–388.

Bassler, J., Hernandez Alvarez, B., Hartmann, M.D., Lupas, A.N., 2015. A domain dictionary of trimeric autotransporter adhesins. Int. J. Med. Microbiol. 305, 265–275.

Bodelon, G., Palomino, C., Fernandez, L.A., 2013. Immunoglobulin domains in Escherichia coli and other enterobacteria: from pathogenesis to applications in antibody technologies. FEMS Microbiol. Rev. 37, 204–250.

Briegel, A., Dias, D.P., Li, Z., Jensen, R.B., Frangakis, A.S., Jensen, G.J., 2006. Multiple large filament bundles observed in Caulobacter crescentus by electron cryotomography. Mol. Microbiol. 62, 5–14.

Brown, J.H., Cohen, C., Parry, D.A., 1996. Heptad breaks in alpha-helical coiled coils: stutters and stammers. Proteins 26, 134–145.

Cabeen, M.T., Charbon, G., Vollmer, W., Born, P., Ausmees, N., Weibel, D.B., Jacobs-Wagner, C., 2009. Bacterial cell curvature through mechanical control of cell growth. EMBO J. 28, 1208–1219.

Cabeen, M.T., Herrmann, H., Jacobs-Wagner, C., 2011. The domain organization of the bacterial intermediate filament-like protein crescentin is important for assembly and function. Cytoskeleton (Hoboken) 68, 205–219.

Conners, R., Hill, D.J., Borodina, E., Agnew, C., Daniell, S.J., Burton, N.M., Sessions, R.B., Clarke, A.R., Catto, L.E., Lammie, D., Wess, T., Brady, R.L., Virji, M., 2008. The Moraxella adhesin UspA1 binds to its human CEACAM1 receptor by a deformable trimeric coiled-coil. EMBO J. 27, 1779–1789.

Crick, F.H.C., 1952. Is alpha-keratin a coiled coil? Nature 170, 882–883.

Crick, F.H.C., 1953a. The Fourier transform of a coiled-coil. Acta Crystallogr. 6, 685–689.

Crick, F.H.C., 1953b. The packing of α-helices: simple coiled-coils. Acta Crystallogr. 6, 689–697.

Fuchino, K., Bagchi, S., Cantlay, S., Sandblad, L., Wu, D., Bergman, J., Kamali-Moghaddam, M., Flardh, K., Ausmees, N., 2013. Dynamic gradients of an intermediate filament-like cytoskeleton are recruited by a polarity landmark during apical growth. Proc. Natl. Acad. Sci. U. S. A. 110, E1889–1897.

Ghosh, P., 2018. Variation, Indispensability, and Masking in the M protein. Trends Microbiol. 26, 132–144.

Hartmann, M.D., 2017. Functional and structural roles of coiled coils. Subcell. Biochem. 82, 63–93.

Hartmann, M.D., Grin, I., Dunin-Horkawicz, S., Deiss, S., Linke, D., Lupas, A.N., Hernandez Alvarez, B., 2012. Complete fiber structures of complex trimeric autotransporter adhesins conserved in enterobacteria. Proc. Natl. Acad. Sci. U. S. A. 109, 20907–20912.

Hartmann, M.D., Mendler, C.T., Bassler, J., Karamichali, I., Ridderbusch, O., Lupas, A.N., Hernandez Alvarez, B., 2016. alpha/beta coiled coils. Elife 5, e11861. https://doi.org/10.7554/eLife.11861.

Hartmann, M.D., Ridderbusch, O., Zeth, K., Albrecht, R., Testa, O., Woolfson, D.N., Sauer, G., Dunin-Horkawicz, S., Lupas, A.N., Alvarez, B.H., 2009. A coiled-coil motif that sequesters ions to the hydrophobic core. Proc. Natl. Acad. Sci. U. S. A. 106, 16950–16955.

Herrmann, H., Haner, M., Brettel, M., Ku, N.O., Aebi, U., 1999. Characterization of distinct early assembly units of different intermediate filament proteins. J. Mol. Biol. 286, 1403–1420.

Hill, D.J., Griffiths, N.J., Borodina, E., Andreae, C.A., Sessions, R.B., Virji, M., 2015. Identification and therapeutic potential of a vitronectin binding region of meningococcal msf. PLoS One 10, e0124133.

Hoiczyk, E., Roggenkamp, A., Reichenbecher, M., Lupas, A., Heesemann, J., 2000. Structure and sequence analysis of Yersinia YadA and Moraxella UspAs reveal a novel class of adhesins. EMBO J. 19, 5989–5999.

Holmes, N.A., Walshaw, J., Leggett, R.M., Thibessard, A., Dalton, K.A., Gillespie, M.D., Hemmings, A.M., Gust, B., Kelemen, G.H., 2013. Coiled-coil protein Scy is a key component of a multiprotein assembly controlling polarized growth in Streptomyces. Proc. Natl. Acad. Sci. U. S. A. 110, E397–406.

Ishikawa, M., Nakatani, H., Hori, K., 2012. AtaA, a new member of the trimeric autotransporter adhesins from Acinetobacter sp. Tol 5 mediating high adhesiveness to various abiotic surfaces. PLoS One 7, e48830.

Kammerer, R.A., Kostrewa, D., Progias, P., Honnappa, S., Avila, D., Lustig, A., Winkler, F.K., Pieters, J., Steinmetz, M.O., 2005. A conserved trimerization motif controls the topology of short coiled coils. Proc. Natl. Acad. Sci. U. S. A. 102 13891-1389.

Kajava, A.V., Squire, J.M., Parry, D.A., 2006. Beta-structures in fibrous proteins. Adv. Protein Chem. 73, 1–15.

Kelemen, G.H., 2017. Intermediate filaments supporting cell shape and growth in Bacteria. Subcell. Biochem. 84, 161–211.

Knappenberger, J.A., Smith, J.E., Thorpe, S.H., Zitzewitz, J.A., Matthews, C.R., 2002. A buried polar residue in the hydrophobic interface of the coiled-coil peptide, GCN4-p1, plays a thermodynamic, not a kinetic role in folding. J. Mol. Biol. 321, 1–6.

Koiwai, K., Hartmann, M.D., Linke, D., Lupas, A.N., Hori, K., 2016. Structural basis for toughness and flexibility in the C-terminal passenger domain of an Acinetobacter

trimeric autotransporter adhesin. J. Biol. Chem. 291, 3705–3724.
Koretke, K.K., Szczesny, P., Gruber, M., Lupas, A.N., 2006. Model structure of the prototypical non-fimbrial adhesin YadA of Yersinia enterocolitica. J. Struct. Biol. 155, 154–161.
Lazar Adler, N.R., Dean, R.E., Saint, R.J., Stevens, M.P., Prior, J.L., Atkins, T.P., Galyov, E.E., 2013. Identification of a predicted trimeric autotransporter adhesin required for biofilm formation of Burkholderia pseudomallei. PLoS One 8, e79461.
Leduc, I., Olsen, B., Elkins, C., 2009. Localization of the domains of the Haemophilus ducreyi trimeric autotransporter DsrA involved in serum resistance and binding to the extracellular matrix proteins fibronectin and vitronectin. Infect. Immun. 77, 657–666.
Leo, J.C., Elovaara, H., Brodsky, B., Skurnik, M., Goldman, A., 2008. The Yersinia adhesin YadA binds to a collagenous triple-helical conformation but without sequence specificity. Protein Eng. Des. Sel. 21, 475–484.
Leo, J.C., Lyskowski, A., Hattula, K., Hartmann, M.D., Schwarz, H., Butcher, S.J., Linke, D., Lupas, A.N., Goldman, A., 2011. The structure of E. Coli IgG-binding protein D suggests a general model for bending and binding in trimeric autotransporter adhesins. Structure 19, 1021–1030.
Liguori, A., Dello Iacono, L., Maruggi, G., Benucci, B., Merola, M., Lo Surdo, P., Lopez-Sagaseta, J., Pizza, M., Malito, E., Bottomley, M.J., 2018. NadA3 structures reveal undecad coiled coils and LOX1 binding regions competed by meningococcus B vaccine-elicited human antibodies. MBio 9.
Linke, D., Riess, T., Autenrieth, I.B., Lupas, A., Kempf, V.A., 2006. Trimeric autotransporter adhesins: variable structure, common function. Trends Microbiol. 14, 264–270.
Lukomski, S., Bachert, B.A., Squeglia, F., Berisio, R., 2017. Collagen-like proteins of pathogenic streptococci. Mol. Microbiol. 103, 919–930.
Lupas, A.N., Bassler, J., Dunin-Horkawicz, S., 2017. The structure and topology of alpha-helical coiled coils. Subcell. Biochem. 82, 95–129.
Lupas, A.N., Gruber, M., 2005. The structure of alpha-helical coiled coils. Adv. Protein Chem. 70, 37–78.
Lyskowski, A., Leo, J.C., Goldman, A., 2011. Structure and biology of trimeric autotransporter adhesins. Adv. Exp. Med. Biol. 715, 143–158.
Malito, E., Biancucci, M., Faleri, A., Ferlenghi, I., Scarselli, M., Maruggi, G., Lo Surdo, P., Veggi, D., Liguori, A., Santini, L., Bertoldi, I., Petracca, R., Marchi, S., Romagnoli, G., Cartocci, E., Vercellino, I., Savino, S., Spraggon, G., Norais, N., Pizza, M., Rappuoli, R., Masignani, V., Bottomley, M.J., 2014. Structure of the meningococcal vaccine antigen NadA and epitope mapping of a bactericidal antibody. Proc. Natl. Acad. Sci. U. S. A. 111, 17128–17133.
McNamara, C., Zinkernagel, A.S., Macheboeuf, P., Cunningham, M.W., Nizet, V., Ghosh, P., 2008. Coiled-coil irregularities and instabilities in group A Streptococcus M1 are required for virulence. Science 319, 1405–1408.
Mil-Homens, D., Pinto, S.N., Matos, R.G., Arraiano, C., Fialho, A.M., 2017. Burkholderia cenocepacia K56-2 trimeric autotransporter adhesin BcaA binds TNFR1 and contributes to induce airway inflammation. Cell. Microbiol. 19.
Oliva, M.A., Halbedel, S., Freund, S.M., Dutow, P., Leonard, T.A., Veprintsev, D.B., Hamoen, L.W., Lowe, J., 2010. Features critical for membrane binding revealed by DivIVA crystal structure. EMBO J. 29, 1988–2001.
Pauling, L., Corey, R.B., 1953. Compound helical configurations of polypeptide chains: structure of proteins of the alpha-keratin type. Nature 171, 59–61.
Paupe, V., Prudent, J., Dassa, E.P., Rendon, O.Z., Shoubridge, E.A., 2015. CCDC90A (MCUR1) is a cytochrome c oxidase assembly factor and not a regulator of the mitochondrial calcium uniporter. Cell Metab. 21, 109–116.
Phillips Jr., G.N., Flicker, P.F., Cohen, C., Manjula, B.N., Fischetti, V.A., 1981. Streptococcal M protein: alpha-helical coiled-coil structure and arrangement on the cell surface. Proc. Natl. Acad. Sci. U. S. A. 78, 4689–4693.
Raghunathan, D., Wells, T.J., Morris, F.C., Shaw, R.K., Bobat, S., Peters, S.E., Paterson, G.K., Jensen, K.T., Leyton, D.L., Blair, J.M., Browning, D.F., Pravin, J., Flores-Langarica, A., Hitchcock, J.R., Moraes, C.T., Piazza, R.M., Maskell, D.J., Webber, M.A., May, R.C., MacLennan, C.A., Piddock, L.J., Cunningham, A.F., Henderson, I.R., 2011. SadA, a trimeric autotransporter from Salmonella enterica serovar Typhimurium, can promote biofilm formation and provides limited protection against infection. Infect. Immun. 79, 4342–4352.
Ruiz-Ranwez, V., Posadas, D.M., Estein, S.M., Abdian, P.L., Martin, F.A., Zorreguieta, A., 2013. The BtaF trimeric autotransporter of Brucella suis is involved in attachment to various surfaces, resistance to serum and virulence. PLoS One 8, e79770.
Singh, B., Su, Y.C., Al-Jubair, T., Mukherjee, O., Hallstrom, T., Morgelin, M., Blom, A.M., Riesbeck, K., 2014. A fine-tuned interaction between trimeric autotransporter haemophilus surface fibrils and vitronectin leads to serum resistance and adherence to respiratory epithelial cells. Infect. Immun. 82, 2378–2389.
Sjolinder, H., Eriksson, J., Maudsdotter, L., Aro, H., Jonsson, A.B., 2008. Meningococcal outer membrane protein NhhA is essential for colonization and disease by preventing phagocytosis and complement attack. Infect. Immun. 76, 5412–5420.
Smeesters, P.R., McMillan, D.J., Sriprakash, K.S., 2010. The streptococcal M protein: a highly versatile molecule. Trends Microbiol. 18, 275–282.
Squeglia, F., Bachert, B., De Simone, A., Lukomski, S., Berisio, R., 2014. The crystal structure of the streptococcal collagen-like protein 2 globular domain from invasive M3-type group A Streptococcus shows significant similarity to immunomodulatory HIV protein gp41. J. Biol. Chem. 289, 5122–5133.
Squire, J.M., Parry, D.A., 2017. Fibrous protein structures: hierarchy, history and heroes. Subcell. Biochem. 82, 1–33.
Stewart, C.M., Buffalo, C.Z., Valderrama, J.A., Henningham, A., Cole, J.N., Nizet, V., Ghosh, P., 2016. Coiled-coil destabilizing residues in the group A Streptococcus M1 protein are required for functional interaction. Proc. Natl. Acad. Sci. U. S. A. 113, 9515–9520.
Szczesny, P., Lupas, A., 2008. Domain annotation of trimeric autotransporter adhesins–daTAA. Bioinformatics 24, 1251–1256.
Tomar, D., Dong, Z., Shanmughapriya, S., Koch, D.A., Thomas, T., Hoffman, N.E., Timbalia, S.A., Goldman, S.J., Breves, S.L., Corbally, D.P., Nemani, N., Fairweather, J.P., Cutri, A.R., Zhang, X., Song, J., Jana, F., Huang, J., Barrero, C., Rabinowitz, J.E., Luongo, T.S., Schumacher, S.M., Rockman, M.E., Dietrich, A., Merali, S., Caplan, J., Stathopulos, P., Ahima, R.S., Cheung, J.Y., Houser, S.R., Koch, W.J., Patel, V., Gohil, V.M., Elrod, J.W., Rajan, S., Madesh, M., 2016. MCUR1 is a scaffold factor for the MCU complex function and promotes mitochondrial bioenergetics. Cell Rep. 15, 1673–1685.
Walshaw, J., Gillespie, M.D., Kelemen, G.H., 2010. A novel coiled-coil repeat variant in a class of bacterial cytoskeletal proteins. J. Struct. Biol. 170, 202–215.
Wang, L., Qin, W., Zhang, J., Bao, C., Zhang, H., Che, Y., Sun, C., Gu, J., Feng, X., Du, C., Han, W., Richard, P.L., Lei, L., 2016. Adh enhances Actinobacillus pleuropneumoniae pathogenicity by binding to OR5M11 and activating p38 which induces apoptosis of PAMs and IL-8 release. Sci. Rep. 6, 24058.
Yeo, H.J., Cotter, S.E., Laarmann, S., Juehne, T., St Geme 3rd, J.W., Waksman, G., 2004. Structural basis for host recognition by the Haemophilus influenzae Hia autotransporter. EMBO J. 23, 1245–1256.
Yu, Z., An, B., Ramshaw, J.A., Brodsky, B., 2014. Bacterial collagen-like proteins that form triple-helical structures. J. Struct. Biol. 186, 451–461.